Pharmaceutical Sciences and Drug Design
ISSN: 3062-4428
2023, Volume 3, Page No: 198-209

Available online at: www.galaxypub.co/page/journals

Galaxy Publication

A Binary Nanoparticle Drug-Delivery System for Leukemia Therapy: Daunorubicin- and Luteolin-Coloaded Nanoparticles Decorated with Aptamer and Transferrin

Noah Hughes[1]*, Layla Campbell[1], Zoe Price[1]

[1]Department of Pharmacognosy, Faculty of Pharmacy, University of California, San Diego, USA.

***E-mail** ✉ noah.hughes.us@outlook.com

Received: 12 January 2023; **Revised:** 09 March 2023; **Accepted:** 11 March 2023

ABSTRACT

This study focused on developing a dual-targeted nanodrug-delivery system functionalized with aptamers (APs) and transferrin (Tf) and co-loaded with daunorubicin (Drn) and luteolin (Lut) for leukemia therapy.AP- and Tf-containing oligonucleotide ligands were individually synthesized. Nanoparticles loaded with Drn and decorated with APs (AP-Drn NPs) and Lut-loaded Tf-functionalized NPs (Tf-Lut NPs) were prepared via self-assembly. These were then combined to form a dual-ligand, dual-drug nanodrug system (AP/Tf-Drn/Lut NPs). The therapeutic efficacy of this system was assessed in vitro using leukemia cell lines and in vivo using a cell-bearing mouse model, compared with single-ligand, single-drug, and free-drug formulations.The AP/Tf-Drn/Lut NPs were spherical, with an average size of 187.3 ± 5.3 nm, and achieved a drug-loading efficiency of approximately 85%. In vitro, the dual-ligand NPs demonstrated significantly higher cytotoxicity than single-ligand counterparts. NPs co-loaded with both drugs exhibited enhanced tumor-cell inhibition relative to single-drug NPs, indicating a synergistic effect. In vivo, AP/Tf-Drn/Lut NPs showed the most potent antileukemic activity with no detectable toxicity.AP/Tf-Drn/Lut NPs represent a promising targeted nanodrug-delivery platform for leukemia therapy, benefiting from the synergistic action of dual drugs, though challenges remain regarding stability during large-scale production and clinical translation.

Keywords: Nanodrug-delivery system, Acute myeloid leukemia, Transferrin, Daunorubicin, Luteolin, Aptamer

How to Cite This Article: Hughes N, Campbell L, Price Z. A Binary Nanoparticle Drug-Delivery System for Leukemia Therapy: Daunorubicin- and Luteolin-Coloaded Nanoparticles Decorated with Aptamer and Transferrin. Pharm Sci Drug Des. 2023;3:198-209. https://doi.org/10.51847/6IKd0GwnbP

Introduction

Acute myeloid leukemia (AML) is a heterogeneous hematologic malignancy and represents the most prevalent form of acute leukemia in adults [1]. The prognosis for AML remains poor, with fewer than 30% of patients surviving five years, and older patients (>65 years) face nearly 90% mortality [2, 3]. Standard AML treatments include chemotherapy regimens, typically combining cytarabine with daunorubicin (Drn) or idarubicin, targeted therapies using FLT3 inhibitors such as midostaurin, quizartinib, and cabozantinib, and immunotherapies like gemtuzumab ozogamicin, an anti-CD33 monoclonal antibody conjugated with calicheamicin [3–6]. However, these approaches are limited by high toxicity, drug resistance, and low patient compliance, highlighting the need for novel therapeutic strategies.

Nanoparticle (NP)-based combination therapies have recently gained attention as promising AML treatments. Clinically, two liposomal formulations are currently available for hematologic malignancies: liposomal Drn (DaunoXome) and liposomal cytarabine plus Drn (CPX-351/VYXEOS) [7, 8]. Phase III trials have demonstrated that the codelivery of Drn and cytarabine via liposomes significantly improves median overall survival (9.56 vs 5.95 months) and overall remission rates (47.7% vs 33.3%) in elderly patients with newly diagnosed high-risk secondary AML compared to free-drug formulations [9], marking a significant advancement in Drn-combination nanoformulation therapy for AML.

Drn, an anthracycline topoisomerase inhibitor, exhibits broad-spectrum activity against AML, adult acute nonlymphocytic leukemia, and pediatric and adult acute lymphocytic leukemia [10]. However, multidrug resistance has restricted its clinical use. Recent research has explored the use of Chinese herbal compounds and NPs to overcome such resistance [11, 12]. Luteolin (Lut; 3′,4′,5,7-tetrahydroxyflavone), a bioactive flavonoid from traditional Chinese medicine, has been applied in treating inflammation, cardiovascular disorders, and cancer [13, 14]. Studies indicate that Lut can enhance the antileukemic effects of chemotherapeutics and counteract multidrug resistance by modulating P-gp and BCL2 upregulation, MCL1 downregulation, and inducing apoptosis in HL60 cells through c-Jun activation and histone H3 acetylation–mediated Fas/FasL expression [15–18]. To date, no literature reports the combined use of Drn and Lut within a single nanoformulation for leukemia therapy, suggesting that such a strategy may enhance cytotoxicity and reduce multidrug resistance.

Aptamers (APs) are oligonucleotides capable of high-affinity, target-specific binding, and AP-based targeting systems have demonstrated potential in AML therapy [19]. APs can specifically recognize AML cell biomarkers, such as CD117, which is highly expressed on these cells [20]. Additionally, AML cells overexpress surface proteins like transferrin (Tf) receptors, enabling Tf-mediated NP targeting [21]. Polyethylene glycol (PEG) serves as a versatile linker, allowing covalent attachment of ligands via its functionalized ends through amide or disulfide bonds [22]. In this study, PEG was utilized to achieve AP and Tf functionalization.

Here, we designed an AP- and Tf-codecorated, Drn- and Lut-coloaded dual nanodrug-delivery system (AP/Tf-Drn/Lut NPs) for AML therapy. Its efficacy was evaluated in vitro using leukemia cell lines and in vivo in a cell-bearing mouse model, compared with single-ligand, single-drug, and free-drug formulations.

Materials and Methods

Drn, Lut, oleic acid (OA), phosphatidylglycerol, human Tf (iron-free), and N-hydroxysuccinimide (NHS) were obtained from Sigma (St. Louis, MO, USA), and (2,3-dioleoyloxy-propyl)-trimethylammonium (DOTAP) was supplied by Avanti Polar Lipids (Birmingham, AL, USA). PEG-COOH (NH2-PEG-COOH) and DSPE-PEG-COOH were purchased from Ponsure Biological (Shanghai, China). The human leukemia cell line HL60 was sourced from the American Type Culture Collection (Manassas, VA, USA) and cultured in DMEM supplemented with 10% FBS at 37°C under 5% CO2.

Animals

Female BALB/c nude mice (4–6 weeks old) were obtained from Beijing Vital River Laboratory Animal Technology (Beijing, China). All in vivo experiments complied with the NIH Guide for the Care and Use of Laboratory Animals and were approved by the Animal Ethics Committee of Qingdao Hospital of Traditional Chinese Medicine.

Synthesis of AP–Polyethylene Glycol–Oleic Acid

PEG-OA was synthesized by dissolving NH2-PEG-COOH and TEA in DMSO, followed by addition to a mixture of OA, DCC, and NHS in DMSO under stirring for 12 h at room temperature [20]. The resulting OA-PEG-COOH was purified via filtration. CD117-specific AP was then conjugated to OA-PEG-COOH to form AP-PEG-OA. OA-PEG-COOH was activated by NHS and reacted overnight with a 5’-amino-modified CD117-specific oligonucleotide AP. AP-PEG-OA conjugates were purified using HPLC, lyophilized to pale-white solids, and confirmed using a BCA protein assay at 562 nm.

Synthesis of Tf-PEG-DSPE

Tf-PEG-DSPE was prepared by forming an amide bond between Tf and DSPE-PEG-COOH [21]. DSPE-PEG-COOH, DCC, and NHS were dissolved in DMSO and stirred for 10 h, followed by addition of Tf and TEA under nitrogen for another 10 h at room temperature. The product was dialyzed, lyophilized, and characterized by infrared and 1H NMR spectroscopy.

Preparation of nanodrug-delivery system

AP-decorated Drn-loaded NPs (AP-Drn NPs) and Tf-Lut NPs were prepared via thin-film dispersion [23]. For AP-Drn NPs, AP-PEG-OA (200 mg) and Drn (100 mg) were dissolved in acetone (5 mL) and evaporated under reduced pressure at 60°C to form a thin film. The film was hydrated with deionized water containing 0.5% DOTAP

to obtain AP-Drn NPs. Tf-Lut NPs were prepared similarly using Tf-PEG-DSPE (200 mg), Lut (100 mg), and phosphatidylglycerol (20 mg), followed by hydration with deionized water.

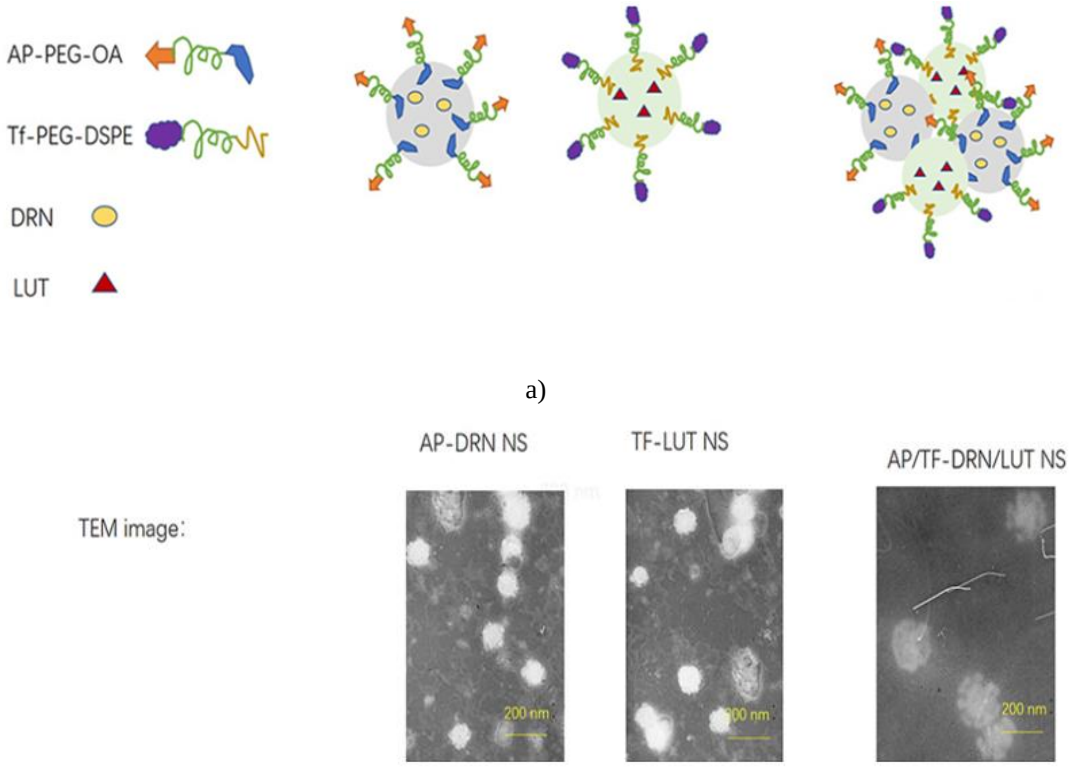

Figure 1. Scheme (a) and TEM images (b) of AP/Tf-Drn/Lut NPs.
Note: AP/Tf-Drn/Lut NPs were nanosized with ligands present on the spherical surface.

AP/Tf-Drn/Lut NPs **(Figure 1a)** were formed via self-assembly [22], in which AP-Drn NPs were combined with Tf-Lut NPs under stirring at 400 rpm. A ligand-only version without drugs (AP/Tf NPs) was prepared similarly but without incorporating drugs. Single-ligand, dual-drug systems—AP-Drn/Lut NPs or Tf-Drn/Lut NPs—were produced using PEG-OA instead of AP-PEG-OA or PEG-DSPE instead of Tf-PEG-DSPE. All nanoparticle formulations were lyophilized and stored at 4°C.

Characterization of nanodrug-delivery system

The surface morphology of AP-Drn NPs, Tf-Lut NPs, and AP/Tf-Drn/Lut NPs was visualized by negative staining with 3% aqueous sodium phosphotungstate and examined using transmission electron microscopy (JEOL, Tokyo, Japan) [24]. Particle size was determined via dynamic light scattering (Beckman Coulter Delsa Nano C, Fullerton, CA), and ζ-potential was measured with a Zetasizer (Malvern Instruments, Malvern, UK). Drn and Lut encapsulation efficiency (EE) and loading content (LC) were quantified by HPLC on a C18 column (150 × 4.6 mm, 12 nm) using a mobile phase of 0.01 M KH2PO4–acetonitrile–acetic acid (45:55:0.27 v:v:v) at 0.5 mL/min, with detection at 350 nm for Lut and 490 nm for Drn [25, 26].

Stability of nanodrug-delivery system

The stability of AP-Drn NPs, Tf-Lut NPs, and AP/Tf-Drn/Lut NPs was evaluated in PBS and DMEM supplemented with 10% FBS. Nanoparticles (20 mg) were incubated in 10 mL of buffer at pH 7.4 and 37°C for 4 days [27]. Changes in particle size and EE were monitored as described above.

In vitro drug release

Drug release profiles were measured using dialysis bags (MWCO 3500 Da) [28]. AP/Tf-Drn/Lut NPs, AP-Drn/Lut NPs, Tf-Drn/Lut NPs, AP-Drn NPs, and Tf-Lut NPs (1 mL each) were placed in PBS (20 mL) containing 0.5% Tween 80, stirred at 100 rpm, and incubated at 37°C. At predetermined intervals, 200 µL samples were collected, and fresh buffer was added. Drn and Lut content was quantified by HPLC.

Cellular uptake

Coumarin 6 was co-loaded with the drugs to evaluate nanoparticle uptake [29]. HL60 cells (10^5 cells/well) were cultured in 24-well plates and incubated with nanoparticles for 1 or 24 h. Cells were washed with D-Hank's solution, collected, centrifuged, and analyzed for uptake efficiency using a BD FACSCalibur flow cytometer.

Cytotoxicity assays

The cytotoxicity of AP/Tf-Drn/Lut NPs and control formulations was measured using MTS assays [30]. HL60 cells were seeded in 96-well plates, incubated overnight, and treated with various nanoparticle formulations or free drugs for 48 h. Afterward, 15 μL of MTS solution was added and incubated for 4 h at 37°C. Cell viability was determined at 490 nm, with survival rates normalized to untreated controls.

Drug combination analysis

The synergistic effect of Drn and Lut was evaluated using the Chou–Talalay method [31]. Combination index at 50% cytotoxicity (CI50) was calculated as CI50 = (D)Drn/(D50)Drn + (D)Lut/(D50)Lut, where (D)Drn and (D)Lut are concentrations in AP/Tf-Drn/Lut NPs achieving 50% inhibition, and (D50)Drn and (D50)Lut correspond to single-drug NPs. CI50 <1, 1, and >1 indicate synergistic, additive, or antagonistic interactions, respectively.

In vivo AML therapy efficiency

HL60 cells (10^6 cells in 150 μL PBS) were subcutaneously injected into BALB/c nude mice to establish a leukemia model. Tumor volume was calculated as $L \times W^2/2$ (L = longest diameter, W = perpendicular diameter) [32]. When tumors reached ~100 mm^3, mice (n=8 per group) were treated intravenously on days 0, 3, 6, 9, 12, 15, 18, and 21 with AP/Tf-Drn/Lut NPs (Drn 5 mg/kg, Lut 2 mg/kg), AP-Drn/Lut NPs, Tf-Drn/Lut NPs, AP-Drn NPs, Tf-Lut NPs, AP/Tf NPs, free Drn/Lut, free Drn, free Lut, or saline. Body weight, creatinine (Cre), alanine aminotransferase (ALT), and WBC counts were monitored.

In vivo pharmacokinetics and biodistribution

Mice were divided into four groups (n=8) and injected with AP/Tf-Drn/Lut NPs, AP-Drn/Lut NPs, Tf-Drn/Lut NPs, or free Drn/Lut (Drn 5 mg/kg and/or Lut 2 mg/kg) [33]. Blood samples were collected at specific time points, centrifuged, and plasma extracted with methanol. Tissues (heart, liver, lung, kidney, spleen, bone marrow, tumor) were harvested at 1 and 48 h, homogenized, and drugs extracted using hexane–diethyl ether (3:1, v:v) before HPLC analysis.

Statistical analysis

Data are expressed as mean ± SD. Differences were assessed using unpaired t-tests or one-way ANOVA via SPSS 19.0, with $P<0.05$ considered significant.

Results and Discussion

Characterization of AP-PEG-OA and Tf-PEG-DSPE

Successful conjugation of AP to PEG-OA was confirmed by enhanced BCA assay at 562 nm, showing two peaks for AP-PEG-OA versus one peak for free AP. Tf-PEG-DSPE formation was verified by IR (3621.3 –NH/–OH, 1898.5 –C=O, 1665.1 –HN–CO–, 1621.7 –HN–CO–) and ^{1}H NMR (CDCl3, 300 MHz δ ppm: 0.89 –CH3, 1.12–1.97 DSPE protons, 2.33 –COCH2–, 2.42 –COCH2CH2–, 2.61 –CH2N–, 3.39 –OCH3–, 3.70–4.10 PEG protons, 5.82 –NH–). Yields were 73.9% for AP-PEG-OA and 78.6% for Tf-PEG-DSPE.

Characterization of nanodrug-delivery system

AP/Tf-Drn/Lut NPs, AP-Drn NPs, and Tf-Lut NPs were spherical **(Figure 1b).** AP/Tf-Drn/Lut NPs measured 187.3 ± 5.3 nm, larger than AP-Drn NPs (91.5 ± 2.8 nm) and Tf-Lut NPs (88.7 ± 2.5 nm). AP-Drn NPs had a positive ζ-potential (18.9 ± 1.7 mV), while the other nanoparticles were negatively charged. Drug encapsulation efficiency exceeded 85% for all formulations. Over 4 days, particle size and EE remained stable **(Figures 2a and 2b)**, consistent with Chen *et al*. [34].

Table 1. Characterization of nanodrug-delivery systems (means ± SD, n=3)

Formulations	Particle size (nm)	PDI	ζ-potential (mV)	Drn		Lut	
				EE (%)	LC (%)	EE (%)	LC (%)
AP/Tf-Drn/Lut NPs	187.3±5.3	0.142±0.019	−25.4±2.6	88.7±3.9	5.2±0.5	85.9±4.2	2.1±0.4
AP-Drn/Lut NPs	186.7±4.7	0.139±0.023	−19.2±2.1	87.5±3.8	5.9±0.6	86.7±3.7	2.4±0.6
Tf-Drn/Lut NPs	188.3±4.5	0.126±0.016	−17.5±1.8	86.5±4.1	5.7±0.6	88.3±3.9	2.2±0.5
AP-Drn NPs	91.5±2.8	0.112±0.011	+18.9±1.7	89.4±4.4	11.8±1.1	/	/
Tf-Lut NPs	88.7±2.5	0.128±0.014	−38.9±3.1	/	/	86.5±3.6	4.6±0.7
AP/Tf NPs	187.8±5.1	0.147±0.026	−37.6±2.9	/	/	/	/

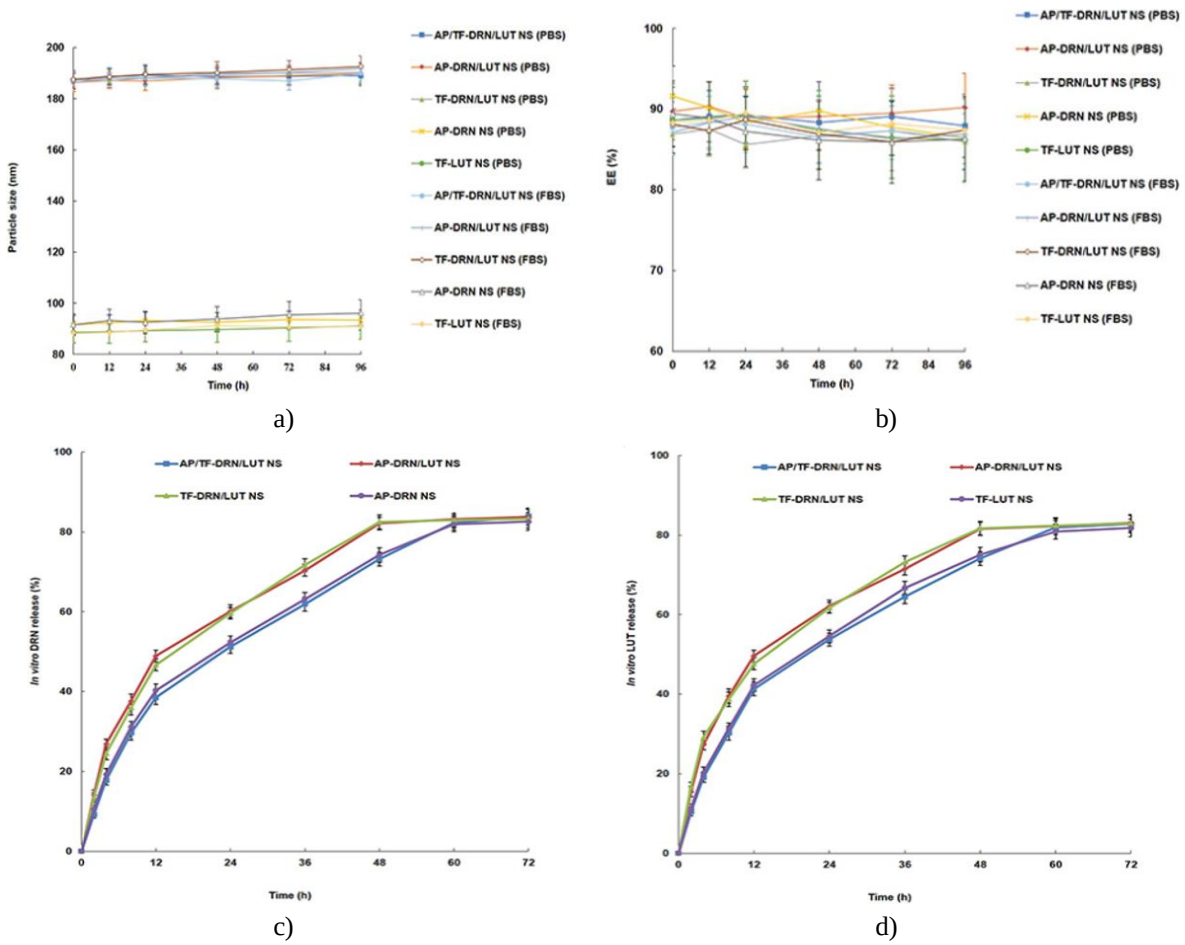

Figure 2. Changes in particle size (a) and encapsulation efficiency (EE) (b) in PBS and culture medium (FBS), and in vitro drug-release profiles of Drn (c) and Lut (d) from nanosystems.

Notes: All samples exhibited sustained drug-release patterns. Data are presented as mean ± SD, n=3.

In vitro release assays

Sustained release was observed for all nanoparticle formulations **(Figures 2c and 2d)**. The dual-ligand AP/Tf-Drn/Lut NPs released drugs more slowly than single-ligand (AP- or Tf-decorated) systems. For example, complete Drn release from AP/Tf-Drn/Lut NPs and AP-Drn NPs occurred after 60 h, whereas AP-Drn/Lut NPs and Tf-Drn/Lut NPs reached full release within 48 h.

Cellular uptake

Cellular uptake results are summarized in **Table 2**. All nanosystems demonstrated high uptake at 1 and 24 h. Notably, dual-ligand AP/Tf-Drn/Lut NPs and AP/Tf NPs exhibited significantly higher uptake than single-ligand systems ($P<0.05$), supporting the enhanced targeting capability of the combined ligands, consistent with previous findings by Jing *et al.* [35].

Table 2. Cellular uptake percentages (means ± SD, n=8)

Formulations	1 h	24 h
AP/Tf-Drn/Lut NPs	73.1±3.6	65.8±3.3
AP-Drn/Lut NPs	59.5±3.2	55.6±2.8
Tf-Drn/Lut NPs	57.1±2.9	54.2±3.1
AP-Drn NPs	60.2±3.3	53.1±2.6
Tf-Lut NPs	58.4±2.7	52.5±2.8
AP/Tf NPs	74.3±3.5	64.7±3.2

Cytotoxicity and drug combination analysis

The AP/Tf-Drn/Lut NPs exhibited markedly greater cytotoxic effects compared with single-ligand formulations, AP-Drn/Lut NPs and Tf-Drn/Lut NPs (P<0.05, **Figure 3**). Both single-ligand dual-drug NPs showed enhanced cell-killing activity relative to free Drn/Lut (P<0.05). Notably, dual-drug, dual-ligand AP/Tf-Drn/Lut NPs outperformed single-drug NPs (AP-Drn or Tf-Lut) in inhibiting tumor cell growth (P<0.05), suggesting a synergistic interaction between Drn and Lut. Supporting this, CI50 calculations **(Table 3)** revealed that a Drn:Lut ratio of 5:2 yielded the lowest CI50 (0.792), indicating optimal synergy, which was adopted for the nanoparticle formulation.

Table 3. CI_{50} values of AP/Tf-Drn/Lut NPs when different Drn:Lut weight ratios were applied (means ± SD, n=8)

Formulations	Drn:Lut (w:w)	IC_{50} of Drn (μM)	IC_{50} of Lut (μM)	CI_{50}
AP-Drn NPs	/	0.93±0.09	/	/
Tf-Lut NPs	/	/	1.16±0.12	/
AP/Tf-Drn/Lut NPs	5:1	0.79±0.08	1.06±0.11	0.987
AP/Tf-Drn/Lut NPs	5:2	0.56±0.05	0.22±0.03	0.792
AP/Tf-Drn/Lut NPs	1:1	0.45±0.04	0.45±0.04	0.872
AP/Tf-Drn/Lut NPs	2:5	0.29±0.03	0.73±0.09	0.941
AP/Tf-Drn/Lut NPs	1:5	0.18±0.02	0.90±0.10	0.969

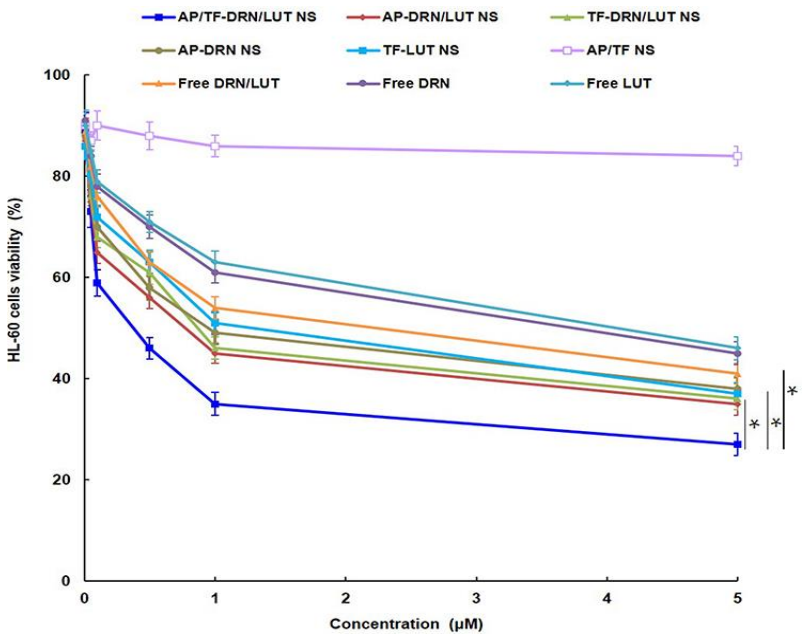

Figure 3. Cytotoxicity of AP/Tf-Drn/Lut NPs and control formulations measured by MTS assay.
Notes: AP/Tf-Drn/Lut NPs showed significantly higher cytotoxicity than single-ligand NPs, single-drug NPs, and free drugs. Data are expressed as mean ± SD, n=6. *P<0.05.

In vivo AML-Therapy efficiency

As shown in **Figure 4a**, all drug-containing formulations significantly inhibited tumor growth compared with saline-treated controls (P<0.05). Among them, AP/Tf-Drn/Lut NPs demonstrated the strongest antileukemic effect relative to single-ligand, single-drug, and free-drug groups (P<0.05). All nanoparticle-based drug systems outperformed free-drug formulations in AML therapy (P<0.05). Body weights of mice treated with drug-loaded NPs remained stable, whereas the saline control and blank NP groups experienced weight reduction (P<0.05, **Figure 4b**). Additionally, treatment with nanoparticles did not induce notable changes in ALT, creatinine, or WBC counts compared with controls, indicating minimal systemic toxicity.

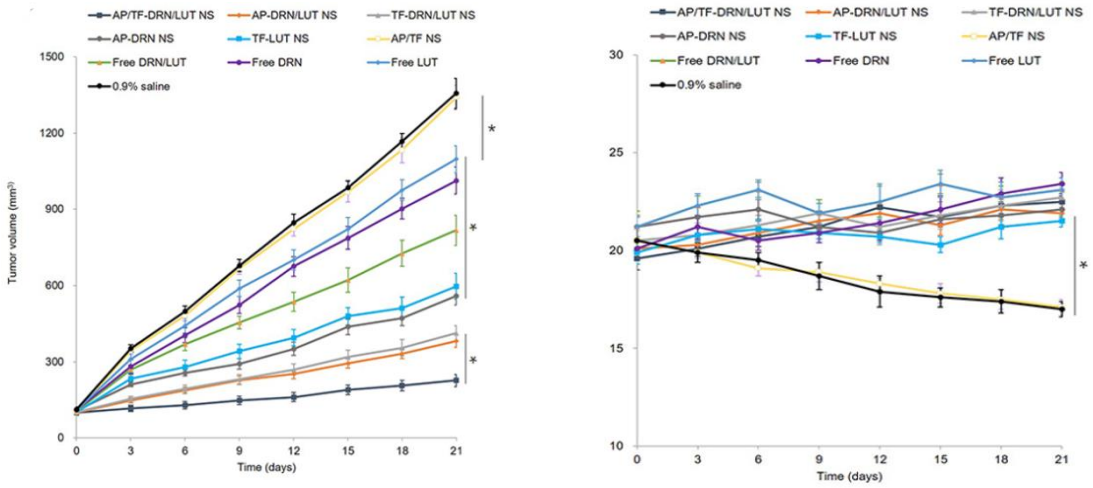

Figure 4. Tumor growth (a) and body weight changes (b) in vivo following AML treatment.

Notes: AP/Tf-Drn/Lut NPs achieved the greatest inhibition of tumor growth compared with single-ligand, single-drug, and free-drug groups. Data are expressed as mean ± SD, n=8. *P<0.05.

In vivo pharmacokinetics and tissue distribution

Pharmacokinetic parameters—including AUC, Cmax, and t½—are presented in **Tables 4 and 5**. For instance, Lut delivered via AP/Tf-Drn/Lut NPs had an AUC of 431.25 ± 11.38 mg·h/L, exceeding that of AP-Drn/Lut NPs (311.26 ± 8.34 mg·h/L), Tf-Drn/Lut NPs (289.86 ± 7.65 mg·h/L), and free Drn/Lut (198.63 ± 4.59 mg·h/L; P<0.05). Similarly, AP/Tf-Drn/Lut NPs showed higher Cmax (55.36 ± 3.21 L/kg·h) and longer t½ (12.37 ± 0.78 h) for Drn compared with the other formulations.

Analysis of drug distribution **(Figure 5)** revealed that AP/Tf-Drn/Lut NPs achieved greater tumor accumulation at 1 and 48 h than single-ligand AP-Drn/Lut NPs and Tf-Drn/Lut NPs (P<0.05), while these single-ligand NPs also outperformed free Drn/Lut (P<0.05). In contrast, free-drug formulations showed higher initial kidney accumulation at 1 h compared with nanoparticle-based systems (P<0.05).

Table 4. Pharmacokinetic parameters for Drn (means ± SD, n=8)

arameters	Unit	AP/Tf-Drn/Lut NPs	AP-Drn/Lut NPs	Tf-Drn/Lut NPs	Free Drn/Lut
C_{max}	L/kg/h	55.36±3.21*	42.31±2.98*	40.55±2.74*	29.83±2.88
$t_{½}$	h	12.37±0.78*	9.72±0.64*	8.84±0.53*	1.89±0.31
AUC_{0-t}	mg/L/h	659.72±19.56*	512.33±17.14*	488.75±21.16*	256.81±9.18
$AUC_{0-\infty}$	mg/L/h	662.31±20.05*	519.64±19.47*	493.23±22.44*	404.73±9.26

Note: *P<0.05 compared with free Drn/Lut.

Abbreviations: C_{max}, plasma drug peak concentration; $t_{½}$, half-life; AUC_{0-t}, area under curve of time 0 to last time point; $AUC_{0-\infty}$, area under curve of time 0 to maximum.

Table 5. Pharmacokinetic parameters for Lut (mean ± SD, n=8)

Parameters	Unit	AP/Tf-Drn/Lut NPs	AP-Drn/Lut NPs	Tf-Drn/Lut NPs	Free Drn/Lut
C_{max}	L/kg/h	35.47±3.18*	28.11±2.36*	26.59±2.95*	18.31±2.12

$t_{½}$	h	8.98±0.58*	5.46±0.41*	5.31±0.34*	1.51±0.29
$AUC_{0–t}$	mg/L/h	431.25±11.38*	311.26±8.34*	289.86±7.65*	198.63±4.59
$AUC_{0–\infty}$	mg/L/h	439.35±12.24*	317.64±11.35*	295.61±6.96*	202.34±5.13

Note: *P<0.05 compared with free Drn/Lut.

Abbreviations: C_{max}, peak plasma drug concentration; $t_{½}$, half-life; $AUC_{0–t}$, area under curve of time 0 to last time point; $AUC_{0–\infty}$, area under curve of time 0 to maximum.

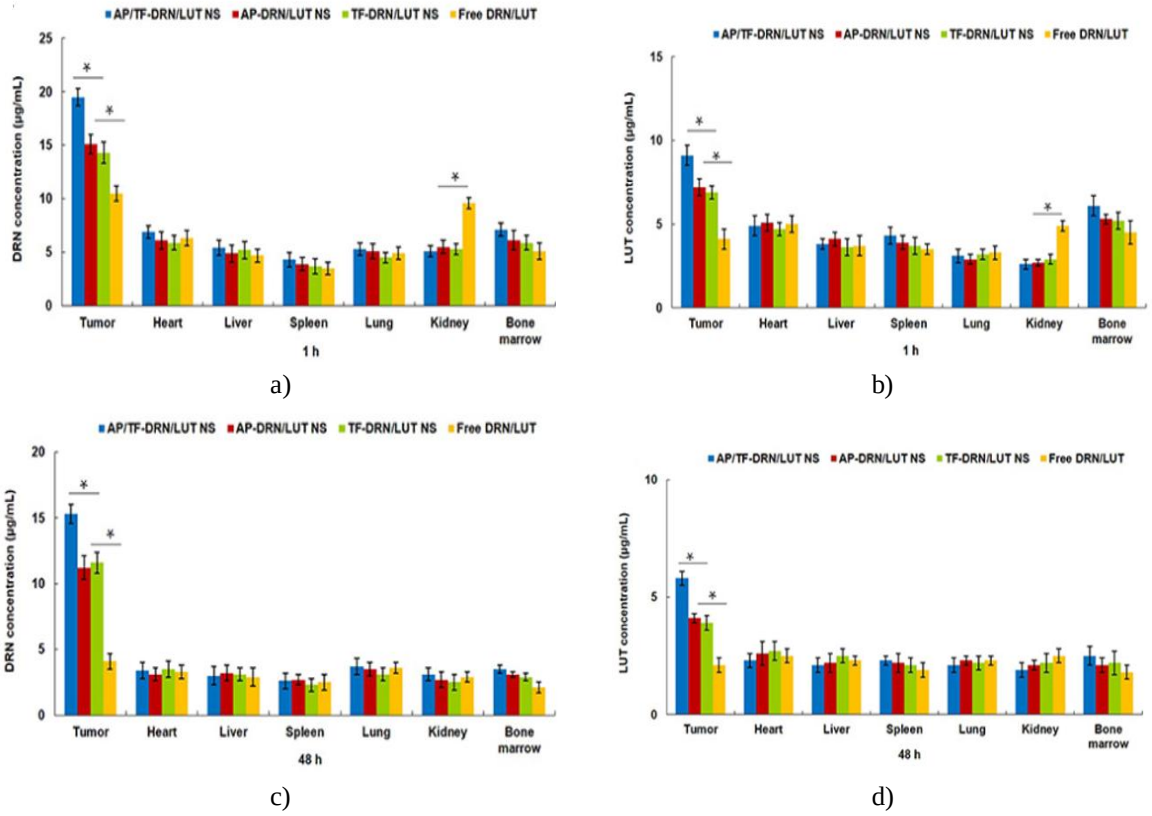

Figure 5. Tissue distribution of Drn (a, c) and Lut (b, d) at 1 h (a, b) and 48 h (c, d) after administration.

Notes: AP/Tf-Drn/Lut NPs exhibited greater tumor accumulation than single-ligand AP-Drn/Lut NPs, Tf-Drn/Lut NPs, and free Drn/Lut. Data are expressed as mean ± SD, n=8. *P<0.05.

This study focused on constructing a dual-ligand nanodrug-delivery system co-loading Drn and Lut for AML treatment. Initially, AP- and Tf-functionalized ligands were synthesized. Cationic AP-Drn NPs and anionic Tf-Lut NPs were prepared separately, then combined via self-assembly driven by electrostatic interactions to form AP/Tf-Drn/Lut NPs [36]. Prior research indicates that solvent composition or ligand electrooxidation can regulate polymer–solvent interactions, enabling diverse NP self-assembly strategies [36]. Similarly, multiresponsive chitosan-based NPs prepared by self-assembly/self-crosslinking have been shown to overcome issues such as low stability and limited drug loading [37]. Dual-ligand, dual-drug NPs have also been applied in targeted cancer therapies, such as docetaxel–formononetin NPs for prostate cancer [38].

The AP/Tf-Drn/Lut NPs were approximately 187 nm in size, aligning with previous findings that particles under 200 nm facilitate tumor accumulation via the enhanced permeability and retention (EPR) effect, reducing systemic toxicity [39]. In vitro, drug release from dual-ligand NPs was slower than from single-ligand systems, likely due to surface ligand density hindering drug diffusion, consistent with other studies [38, 40].

Cytotoxicity assays revealed that AP/Tf-Drn/Lut NPs had superior cell-killing effects compared with single-ligand dual-drug NPs, reflecting enhanced targeting and intracellular accumulation [41]. Dual-drug NPs also showed higher tumor inhibition than single-drug NPs, indicating synergism. CI50 analysis using the Chou–Talalay method confirmed the optimal Drn:Lut ratio of 5:2 for synergy (CI50 = 0.46), which guided nanoparticle formulation [42, 43].

Pharmacokinetic and biodistribution studies demonstrated that AP/Tf-Drn/Lut NPs achieved higher AUC, Cmax, t½, and tumor accumulation, reflecting prolonged circulation and effective targeting [44, 45]. Tumor enrichment

is attributed to leaky vasculature and nanoscale size permitting passive targeting via the EPR effect [46]. Reduced renal accumulation minimized potential nephrotoxicity, enhancing overall therapeutic efficacy [47].

Prior reports indicate that dual-ligand NPs can improve AML treatment while reducing systemic toxicity [48, 49]. Consistent with these findings, AP/Tf-Drn/Lut NPs achieved superior tumor suppression with minimal impact on body weight, compared with controls where weight loss was observed due to treatment-related stress [50, 51].

Conclusion

AP/Tf-Drn/Lut NPs exhibited significantly higher cytotoxicity than single-ligand formulations, and dual-drug loading provided enhanced tumor-cell inhibition via a synergistic effect. In vivo, these NPs achieved potent antileukemic activity without evident toxicity, supporting their potential as a targeted therapy for AML. Limitations include challenges in large-scale production and translation from laboratory to clinical application.

Acknowledgments: None

Conflict of Interest: None

Financial Support: None

Ethics Statement: None

References

1. Estey E, Döhner H. Acute myeloid leukaemia. Lancet. 2006;368(9550):1894–907. doi:10.1016/S0140-6736(06)69780-8
2. Daver N, Schlenk RF, Russell NH, Levis MJ. Targeting FLT3 mutations in AML: review of current knowledge and evidence. Leukemia. 2019;33(2):299–312. doi:10.1038/s41375-018-0357-9
3. Huang X, Lin H, Huang F, Xie Y, Wong KH, Chen X, et al. Targeting Approaches of Nanomedicines in Acute Myeloid Leukemia. Dose Response. 2019;17(4):1559325819887048. doi:10.1177/1559325819887048. PMID: 31853234; PMCID: PMC6906351.
4. Ferrara F, Vitagliano O. Induction therapy in acute myeloid leukemia: is it time to put aside standard 3 + 7? Hematol Oncol. 2019;37(5):558–63. doi:10.1002/hon.2615
5. Lin M, Chen B. Advances in the drug therapies of acute myeloid leukemia (except acute wpromyelocytic leukemia). Drug Des Devel Ther. 2018;12:1009–17. doi:10.2147/DDDT.S161199
6. Norsworthy KJ, Ko CW, Lee JE, Liu J, John CS, Przepiorka D, et al. FDA Approval Summary: mylotarg for treatment of patients with relapsed or refractory CD33-Positive acute myeloid leukemia. Oncologist. 2018;23(9):1103-8. doi:10.1634/theoncologist.2017-0604. Epub 2018 Apr 12. PMID: 29650683; PMCID: PMC6192608.
7. Latagliata R, Breccia M, Fazi P, Iacobelli S, Martinelli G, Di Raimondo F, et al. Liposomal daunorubicin versus standard daunorubicin: long term follow-up of the GIMEMA GSI 103 AMLE randomized trial in patients older than 60 years with acute myelogenous leukaemia. Br J Haematol. 2008;143(5):681-9. doi:10.1111/j.1365-2141.2008.07400.x. Epub 2008 Oct 20. PMID: 18950458.
8. 8. Maakaron JE, Mims AS. Daunorubicin-cytarabine liposome (CPX-351) in the management of newly diagnosed secondary AML: a new twist on an old cocktail. Best Pract Res Clin Haematol. 2019;32(2):127–33. doi:10.1016/j.beha.2019.05.005
9. Lancet JE, Uy GL, Cortes JE, Newell LF, Lin TL, Ritchie EK, et al. CPX-351 (cytarabine and daunorubicin) liposome for injection versus conventional cytarabine plus daunorubicin in older patients with newly diagnosed secondary acute myeloid leukemia. J Clin Oncol. 2018;36(26):2684-92. doi:10.1200/JCO.2017.77.6112. Epub 2018 Jul 19. PMID: 30024784; PMCID: PMC6127025.
10. Kaspers GJ, Zimmermann M, Reinhardt D, Gibson BE, Tamminga RY, Aleinikova O, et al. Improved outcome in pediatric relapsed acute myeloid leukemia: results of a randomized trial on liposomal daunorubicin by the International BFM Study Group. J Clin Oncol. 2013;31(5):599-607. doi:10.1200/JCO.2012.43.7384. Epub 2013 Jan 14. PMID: 23319696.

11. Jin J, Wang FP, Wei H, Liu G. Reversal of multidrug resistance of cancer through inhibition of P-glycoprotein by 5-bromotetrandrine. Cancer Chemother Pharmacol. 2005;55(2):179–88. doi:10.1007/s00280-004-0868-0
12. Hu CM, Zhang L. Nanoparticle-based combination therapy toward overcoming drug resistance in cancer. Biochem Pharmacol. 2012;83(8):1104–11. doi:10.1016/j.bcp.2012.01.008
13. Kim YS, Kim SH, Shin J, Harikishore A, Lim JK, Jung Y, et al. Luteolin suppresses cancer cell proliferation by targeting vaccinia-related kinase 1. PLoS One. 2014 ;9(10):109655. doi:10.1371/journal.pone.0109655. PMID: 25310002; PMCID: PMC4195671.
14. Chian S, Li YY, Wang XJ, Tang XW. Luteolin sensitizes two oxaliplatin-resistant colorectal cancer cell lines to chemotherapeutic drugs via inhibition of the Nrf2 pathway. Asian Pac J Cancer Prev. 2014;15(6):2911–6. doi:10.7314/APJCP.2014.15.6.2911
15. Zheng CH, Zhang M, Chen H, Wang CQ, Zhang MM, Jiang JH, et al. Luteolin from flos chrysanthemi and its derivatives: new small molecule Bcl-2 protein inhibitors. Bioorg Med Chem Lett. 2014;24(19):4672-7. doi:10.1016/j.bmcl.2014.08.034. Epub 2014 Aug 20. PMID: 25193233.
16. Danışman Kalındemirtaş F, Birman H, Candöken E, Bilgiş Gazioğlu S, Melikoğlu G, Kuruca S. Cytotoxic effects of some flavonoids and imatinib on the K562 chronic myeloid leukemia cell line: data analysis using the combination index method. Balkan Med J. 2019;36(2):96–105. doi:10.4274/balkanmedj.galenos.2018.2017.1244
17. Chen PY, Tien HJ, Chen SF, Horng CT, Tang HL, Jung HL, et al. Response of myeloid leukemia cells to luteolin is modulated by differentially expressed pituitary tumor-transforming gene 1 (PTTG1) oncoprotein. Int J Mol Sci. 2018;19(4):1173. doi:10.3390/ijms19041173. PMID: 29649138; PMCID: PMC5979486.
18. Polier G, Giaisi M, Köhler R, Müller WW, Lutz C, Buss EC, et al. Targeting CDK9 by wogonin and related natural flavones potentiates the anti-cancer efficacy of the Bcl-2 family inhibitor ABT-263. Int J Cancer. 2015;136(3):688-98. doi:10.1002/ijc.29009. Epub 2014 Jun 13. PMID: 24895203.
19. Wang M, Wu H, Duan M, Yang Y, Wang G, Che F, et al. SS30, a novel thioaptamer targeting CD123, inhibits the growth of acute myeloid leukemia cells. Life Sci. 2019;232:116663. doi:10.1016/j.lfs.2019.116663. Epub 2019 Jul 16. Erratum in: Life Sci. 2020;240:117111. doi:10.1016/j.lfs.2019.117111. PMID: 31323275.
20. Zhao N, Pei SN, Qi J, Zeng Z, Iyer SP, Lin P, et al. Oligonucleotide aptamer-drug conjugates for targeted therapy of acute myeloid leukemia. Biomaterials. 2015;67:42-51. doi:10.1016/j.biomaterials.2015.07.025. Epub 2015 Jul 15. PMID: 26204224; PMCID: PMC4550516.
21. Kim TH, Jo YG, Jiang HH, Lim SM, Youn YS, Lee S, et al. PEG-transferrin conjugated TRAIL (TNF-related apoptosis-inducing ligand) for therapeutic tumor targeting. J Control Release. 2012;162(2):422-8. doi:10.1016/j.jconrel.2012.07.021. Epub 2012 Jul 21. PMID: 22824780; PMCID: PMC3629958.
22. Van Vlerken LE, Vyas TK, Amiji MM. Poly (ethylene glycol)-modified nanocarriers for tumor-targeted and intracellular delivery. Pharm Res. 2007;24(8):1405–14. doi:10.1007/s11095-007-9284-6
23. Nguyen CT, Tran TH, Amiji M, Lu X, Kasi RM. Redox-sensitive nanoparticles from amphiphilic cholesterol-based block copolymers for enhanced tumor intracellular release of doxorubicin. Nanomedicine. 2015;11(8):2071–82. doi:10.1016/j.nano.2015.06.011
24. Mao K, Zhang W, Yu L, Yu Y, Liu H, Zhang X. Transferrin-decorated protein-lipid hybrid nanoparticle efficiently delivers cisplatin and docetaxel for targeted lung cancer treatment. Drug Des Devel Ther. 2021;15:3475–86. doi:10.2147/DDDT.S296253
25. El-Lakany SA, Elzoghby AO, Elgindy NA, Hamdy DA. HPLC methods for quantitation of exemestane–luteolin and exemestane–resveratrol mixtures in nanoformulations. J Chromatogr Sci. 2016;54(8):1282–9. doi:10.1093/chromsci/bmw063
26. Yue Y, Eun JS, Lee MK, Seo SY. Synthesis and characterization of G5 PAMAM dendrimer containing daunorubicin for targeting cancer cells. Arch Pharm Res. 2012;35(2):343–9. doi:10.1007/s12272-012-0215-7
27. Wu R, Zhang Z, Wang B, Chen G, Zhang Y, Deng H, et al. Combination chemotherapy of lung cancer - Co-Delivery of docetaxel prodrug and cisplatin using aptamer-decorated lipid-polymer hybrid nanoparticles. Drug Des Devel Ther. 2020;14:2249-61. doi:10.2147/DDDT.S246574. PMID: 32606595; PMCID: PMC7293388.
28. Wu C, Xu Q, Chen X, Liu J. Delivery luteolin with folacin-modified nanoparticle for glioma therapy. Int J Nanomedicine. 2019;14:7515–31. doi:10.2147/IJN.S214585

29. Fan X, Wang T, Ji Z, Li Q, Shen H, Wang J. Synergistic combination therapy of lung cancer using lipid-layered cisplatin and oridonin co-encapsulated nanoparticles. Biomed Pharmacother. 2021;141:111830. doi:10.1016/j.biopha.2021.111830
30. Haghighi FH, Binaymotlagh R, Mirahmadi-Zare SZ, Hadadzadeh H. Aptamer/magnetic nanoparticles decorated with fluorescent gold nanoclusters for selective detection and collection of human promyelocytic leukemia (HL-60) cells from a mixture. Nanotechnology. 2020;31(2):025605. doi:10.1088/1361-6528/ab484a
31. Chou TC. Drug combination studies and their synergy quantification using the Chou-Talalay method. Cancer Res. 2010;70(2):440–6. doi:10.1158/0008-5472.CAN-09-1947
32. Truebenbach I, Kern S, Loy DM, Höhn M, Gorges J, Kazmaier U, et al. Combination Chemotherapy of L1210 Tumors in Mice with Pretubulysin and Methotrexate Lipo-Oligomer Nanoparticles. Mol Pharm. 2019;16(6):2405-17. doi:10.1021/acs.molpharmaceut.9b00038. Epub 2019 May 13. PMID: 31025870.
33. Bao H, Zheng N, Li Z, Zhi Y. Synergistic effect of tangeretin and atorvastatin for colon cancer combination therapy: targeted delivery of these dual drugs using RGD peptide decorated nanocarriers. Drug Des Devel Ther. 2020;14:3057–68. doi:10.2147/DDDT.S256636
34. Chen Y, Xu Z, Lu T, Luo J, Xue H. Prostate-specific membrane antigen targeted, glutathione-sensitive nanoparticles loaded with docetaxel and enzalutamide for the delivery to prostate cancer. Drug Deliv. 2022;29(1):2705–12. doi:10.1080/10717544.2022.2110998
35. Jing F, Li J, Liu D, Wang C, Sui Z. Dual ligands modified double targeted nano-system for liver targeted gene delivery. Pharm Biol. 2013;51(5):643–9. doi:10.3109/13880209.2012.761245
36. Choueiri RM, Klinkova A, Pearce S, Manners I, Kumacheva E. Self-assembly and surface patterning of polyferrocenylsilane-functionalized gold nanoparticles. Macromol Rapid Commun. 2018;39(3). doi:10.1002/marc.201700554
37. Yang Z, Li P, Chen Y, Gan Q, Feng Z, Jin Y, et al. Construction of pH/glutathione responsive chitosan nanoparticles by a self-assembly/self-crosslinking method for photodynamic therapy. Int J Biol Macromol. 2021;167:46-58. doi:10.1016/j.ijbiomac.2020.11.141. Epub 2020 Nov 30. PMID: 33271181.
38. Dong Z, Wang Y, Guo J, Tian C, Pan W, Wang H, et al. Prostate cancer therapy using docetaxel and formononetin combination: hyaluronic acid and epidermal growth factor receptor targeted peptide dual ligands modified binary nanoparticles to facilitate the in vivo anti-tumor activity. Drug Des Devel Ther. 2022;16:2683-93. doi:10.2147/DDDT.S366622. PMID: 35983428; PMCID: PMC9380734.
39. Zhang R, Ru Y, Gao Y, Li J, Mao S. Layer-by-layer nanoparticles co-loading gemcitabine and platinum (IV) prodrugs for synergistic combination therapy of lung cancer. Drug Des Devel Ther. 2017;11:2631–42. doi:10.2147/DDDT.S143047
40. Pang J, Xing H, Sun Y, Feng S, Wang S. Non-small cell lung cancer combination therapy: hyaluronic acid modified, epidermal growth factor receptor targeted, pH sensitive lipid-polymer hybrid nanoparticles for the delivery of erlotinib plus bevacizumab. Biomed Pharmacother. 2020;125:109861. doi:10.1016/j.biopha.2020.109861
41. Wang H, Sun G, Zhang Z, Ou Y. Transcription activator, hyaluronic acid and tocopheryl succinate multi-functionalized novel lipid carriers encapsulating etoposide for lymphoma therapy. Biomed Pharmacother. 2017;91:241–50. doi:10.1016/j.biopha.2017.04.104
42. Li S, Wang L, Li N, Liu Y, Su H. Combination lung cancer chemotherapy: design of a pH-sensitive transferrin-PEG-Hz-lipid conjugate for the co-delivery of docetaxel and baicalin. Biomed Pharmacother. 2017;95:548–55. doi:10.1016/j.biopha.2017.08.090
43. Chou TC. Theoretical basis, experimental design, and computerized simulation of synergism and antagonism in drug combination studies. Pharmacol Rev. 2006;58(3):621–81. doi:10.1124/pr.58.3.10
44. Wang B, Hu W, Yan H, Chen G, Zhang Y, Mao J, et al. Lung cancer chemotherapy using nanoparticles: enhanced target ability of redox-responsive and pH-sensitive cisplatin prodrug and paclitaxel. Biomed Pharmacother. 2021;136:111249. doi:10.1016/j.biopha.2021.111249. Epub 2021 Jan 12. PMID: 33450493.
45. Jedrzejczyk M, Wisniewska K, Kania KD, Marczak A, Szwed M. Transferrin-bound doxorubicin enhances apoptosis and DNA damage through the generation of pro-inflammatory responses in human leukemia cells. Int J Mol Sci. 2020;21(24):9390. doi:10.3390/ijms21249390

46. Choi J, Ko E, Chung HK, Lee JH, Ju EJ, Lim HK, et al. Nanoparticulated docetaxel exerts enhanced anticancer efficacy and overcomes existing limitations of traditional drugs. Int J Nanomedicine. 2015;10:6121-32. doi:10.2147/IJN.S88375. PMID: 26457052; PMCID: PMC4598197.
47. Li C, Ge X, Wang L. Construction and comparison of different nanocarriers for co-delivery of cisplatin and curcumin: a synergistic combination nanotherapy for cervical cancer. Biomed Pharmacother. 2017;86:628–36. doi:10.1016/j.biopha.2016.12.042
48. Zhu B, Zhang H, Yu L. Novel transferrin modified and doxorubicin loaded pluronic 85/lipid-polymeric nanoparticles for the treatment of leukemia: in vitro and in vivo therapeutic effect evaluation. Biomed Pharmacother. 2017;86:547–54. doi:10.1016/j.biopha.2016.11.121
49. He F, Wen N, Xiao D, Yan J, Xiong H, Cai S, et al. Aptamer-Based targeted drug delivery systems: current potential and challenges. Curr Med Chem. 2020;27(13):2189-219. doi:10.2174/0929867325666181008142831. PMID: 30295183.
50. Wang L, Wang W, Rui Z, Zhou D. The effective combination therapy against human osteosarcoma: doxorubicin plus curcumin co-encapsulated lipid-coated polymeric nanoparticulate drug delivery system. Drug Deliv. 2016;23(9):3200–8. doi:10.3109/10717544.2016.1162875
51. Liu B, Han L, Liu J, Han S, Chen Z, Jiang L. Co-delivery of paclitaxel and TOS-cisplatin via TAT-targeted solid lipid nanoparticles with synergistic antitumor activity against cervical cancer. Int J Nanomedicine. 2017;12:955–68. doi:10.2147/IJN.S115136